Optical and structural properties of WO_3 as a function of the annealing temperature

J. DIAZ-REYES[1,a] , J. E. FLORES-MENA[2], J. M. GUTIERREZ-ARIAS [2], M. M. MORIN-CASTILLO[2], H. AZUCENA-COYOTECATL [2], M. GALVÁN[3], P. RODRIGUEZ-FRAGOSO[4], A. MENDEZ-LÓPEZ[5]

[1] CIBA-IPN, Ex-Hacienda de San Molino Km. 1.5. Tepetitla, Tlaxcala. 90700. MEXICO

[2] FCE-BUAP, Av. San Claudio y 18 Sur, Jardines de San Manuel, CU, Puebla, Pue., 72570, MEXICO

[3] Depto. de Ing. Eléctrica, SEES. CINVESTAV-IPN. A. Postal 14-740. México, D. F. 07000. MÉXICO

[4] Depto. de Física. CINVESTAV-IPN. A. Postal 14-740. México, D. F. 07000. MÉXICO

[5] CIDS-ICUAP, BUAP. CU, Edif. No. 137. Col. San Manuel. Puebla, Pue. 72570. MÉXICO

[a] jdiazr2010@yahoo.com,

Abstract: - This work presents a study of effect of annealing temperature on optical and structural properties of WO_3 that has been deposited by hot-filament metal oxide deposition (HFMOD). X-ray diffraction shows that the as-deposited WO_3 films present mainly monoclinic crystalline phase. The Raman spectrum shows four intense peaks that are typical Raman peaks of crystalline WO_3 (m-phase) that corresponds to the stretching vibrations of the bridging oxygen that enhance and increase their intensity with the annealing temperature. Band gap can be varied from 2.92 to 3.15 eV by annealing WO_3 from 0 to 500 ºC. The photoluminescence response of the as-deposited film presents two radiative transitions centered at 2.04 and 2.65 eV that are associated to oxygen vacancies.

Key-Words: - Compound semiconductors; HFMOD; Novel Materials and Technological Advances for electrochromics; semiconductors growth; WO_3 semiconductors; XPS, Raman spectroscopy, X-ray, Transmittance spectroscopy

1 Introduction

Transition metal oxides represent a large family of materials possessing various interesting properties, such as superconductivity, colossal magneto-resistance and piezoelectricity. Among them, tungsten oxide is of intense interest and has been investigated extensively for its distinctive properties. With outstanding electrochromic [1], photochromic [2], gaschromic [3], gas sensor [4], photo-catalyst [5] and photoluminescence properties [6], tungsten oxide has been used to construct `smart-window', anti-glare rear view mirrors for automobiles, non-emissive displays, optical recording devices, solid-state gas sensors, humidity and temperature sensors, biosensors, photonic crystals and so forth. WO_3 thin films can be prepared by various deposition techniques such as thermal evaporation [3,7], spray pyrolysis [8], sputtering [9], pulsed laser ablation [4], sol–gel coating [10] and chemical vapour deposition [11].

The purpose of this work is to characterize the WO_3 layers deposited by hot filament metal oxide deposition (HFMOD) technique, which were annealed wide temperature range. This growth technique has some advantage compared the conventional growth technique, it is easily implemented and it is not expensive. The investigations so far carried out in our laboratory show that the films can be deposited with a good stoichiometric control, with relatively high deposition rates and present good adhesion to both metallic and dielectric substrates. The characterization of the deposited material is carried out by XPS, X-ray, Raman spectroscopy and transmittance.

2 Experimental details

The WO_3 thin films were deposited by hot-Filament Metal Oxide Deposition (HFMOD) technique at atmospheric pressure on corning glass at room temperature; its main characteristics have been reported in the literature [12]. For determining the chemical stoichiometry was used X-ray Photoelectron Spectroscopy (XPS). For the XPS analyses, a hemispherical spectrometer using the unmonochromatized Kα X-ray line of aluminum was employed. To investigate the possible tungsten valence states, the 4f-doublet peak or the 3d-doublet

peak, respectively, were fitted with Gaussian peaks corresponding to known bonding states of tungsten and oxygen. The crystalline phase and structure was determined with a Bruker D8 Discover diffractometer using the copper Kα radiation (1.5406 Å) at 40 kV and 40 mA with parallel beam geometry. Raman scattering experiments were performed at room temperature using the 6328 Å line of a He-Ne laser at normal incidence for excitation. The laser light was focused to a diameter of 6.0 μm at the sample using a 50x (numerical aperture 0.9) microscope objective. The nominal laser power used in these measurements was 20 mW. Scattered light was analyzed using a micro-Raman system (Lambram model of Dilor), a holographic notch filter made by Kaiser Optical System, Inc. (model superNotch-Plus), a 256x1024-pixel CCD used as detector cooled to 140 K using liquid nitrogen, and two interchangeable gratings (600 and 1800 g/mm). Typical spectrum acquisition time was limited to 60 s to minimize the sample heating effects. Absolute spectral feature position calibration to better than 0.5 cm^{-1} was performed using the observed position of Si which is shifted by 521.2 cm^{-1} from the excitation line.

Mathematical Equations must be numbered as follows: (1), (2), …, (99) and not (1.1), (1.2),…, (2.1), (2.2),… depending on your various Sections.

3 Results and discussion

Figure 1 shows the evolution of the W(4f) doublet peak of WO_3 deposited before and after 500ºC treatment, here XPS is used to find the chemical stoichiometry and confirm that the film is composed by WO_3. They have the same characteristics as bulk WO_3. Fig. 1(a) shows the W(4f) core level spectra recorded on the as-deposited WO_3 sample, and the results of its fitting analysis. To reproduce the experimental data, one doublet function was used for the W(4f) component. This contains W($4f_{7/2}$) at 35.6 eV and W($4f_{5/2}$) at 37.8 eV with a full-width at half-maximum (FWHM) of 1.75 eV. The area ratio of these two peaks is 0.75, which is supported by the spin–orbit splitting theory of 4f levels. Moreover, the structure was shifted by 5.0 eV towards higher energy relative to the metal state. It is thus clear that the main peaks in the XPS spectrum are attributed to the W^{6+} state on the surface [13,14], indicating that the film is composed of stoichiometric WO_3. In stoichiometric WO_3, the six valence electrons of the tungsten atom are transferred into the oxygen p-like bands, which are thus completely filled. In this case, the tungsten 5d valence electrons have no part of their wavefunction near the tungsten atom and the remaining electrons in the tungsten atom experience a stronger Coulomb interaction with the nucleus than in the case of a tungsten atom in a metal, in which the screening of the nucleus has a component due to the 5d valence electrons. Therefore, the binding energy of the W(4f) level is larger in WO_3 than in metallic tungsten. If an oxygen vacancy exists, the electronic density near its adjacent W atom increases, the screening of its nucleus is higher and, thus, the 4f level energy is expected to be at a lower binding energy [13]. After annealing at 400ºC in air all peaks had a slight shift in the direction of low energy. By increasing the annealing temperature, it was observed that the position of the W(4f) peak did not change appreciably up to temperatures lower than 400ºC, which indicates that the films only improve their crystalline quality. But for WO_3 thin film annealed at 500°C, the W(4f) peak moved to a lower binding energy so that the W($4f_{7/2}$) position was observed at 35.0 eV. This can be related to oxygen vacancies at this high annealing temperature and the formation of W^{5+}.

As-deposited WO_3 films present mainly the monoclinic crystalline phase and a small fraction of orthorhombic crystalline phase that obtained by X-ray diffraction. The X-ray patterns of as-deposited WO_3 film on glass, and whose lattice parameters were calculated using the software DICVOL04, obtaining the following lattice parameters values: a= 3.8465 Å, b= 7.5449 Å, c= 7.3066 Å, β= 90.924° and its unit lattice volume is about 212.02 $Å^3$, further the annealing films are shown in Fig. 2. The XRD patterns obtained of the as-deposited sample and the annealed samples are quite similar, which indicates clearly that the WO_3 does not change of crystalline phase with the annealing in the investigated temperature range. As is seen in Fig. 2, the intensity increases as the annealing temperature increases up to 400ºC, in which the material has a better quality crystalline, and it undergoes a decrement of the intensity indicated a lower crystalline quality, as was found by XPS measurements due to the loss of oxygen by annealing one.

The Raman spectrum of as-deposited WO_3 film shows mainly seven vibrational bands in range of 50-1000 cm^{-1} centered at 801, 710, 322, 262, 126, 81 and 65 cm^{-1}. As has been reported in the literature the Raman bands sited in the range 750 - 950 cm^{-1} are attributed to either the antisymmetric stretch of M-O-M bonds (i. e., ν_{as} [M-O-M]) or the symmetric stretch of (-O-M-O-) bonds (i. e., ν_s [-O-M-O-]) [15]). Most peaks below 200 cm^{-1} are attributed to lattice modes, whereas the mid and high frequency regions correspond to deformation and stretching modes, respectively. Thus, the intense peaks centered at 801 and 710 cm^{-1} are typical Raman peaks of crystalline

WO_3 (m-phase), which correspond to the stretching vibrations of the bridging oxygen [16,17] and these are assigned to W-O stretching (ν), W-O bending (δ) and O-W-O deformation (γ) modes, respectively [18,19]. In Fig. 4a illustrates the Raman spectrum in the range from 50 to 120 cm^{-1} for the as-deposited sample. It presents the typical characteristic peaks of the monoclinic crystalline phase at low frequencies that were obtained by deconvolution using Lorentzian curves for finding the peaks frequency that are associated to lattice modes [20,21]. Similar vibration modes were obtained by Raman theories and are in agreement with the results of de Wijs *et al.* [17]. The sharp peaks at 262 and 322 cm^{-1} are assigned to the bending vibration δ(O-W-O) [18, 20]. The Raman peak sited at 262 cm^{-1} is enough intense, which means that a great fraction of crystalline phase is present in the as-deposited films. The 801, 710 and 262 cm^{-1} are very intense and typical modes of the crystalline WO_3 film. All these peaks are in good agreement with what has been published on WO_3 obtained by conventional techniques.

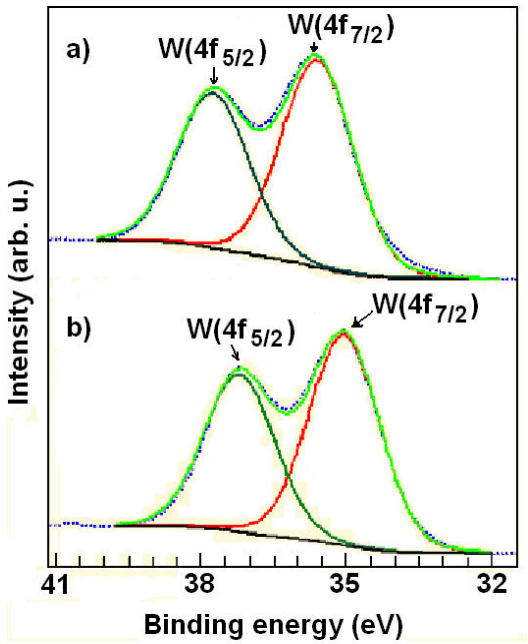

Fig. 1. W (4f) core level spectra of WO_3 thin films: (a) as-deposited and (b) annealed at 500ºC.

For corroborating the above discussed results, the WO_3 samples were annealed at different temperatures in the range from 100 to 500 C during 10 min in a nitrogen atmosphere. The Raman spectra of the samples annealed at 400 and 500ºC are shown in Fig. 3. Before and after annealing the films show a similar Raman curve [22]. Small variations of the intensity between the spectra are found in all the range. All the background from the underlying glass slide in the spectra decreases after annealing of 300ºC, that is, the I_R/I_N ratio of Raman intensity (I_R) and noisy signal intensity (I_N) increased after annealing. In particular, the Raman spectrum at lo frequencies of the annealed sample at 500ºC presents the same peaks than the spectrum of the as-deposited one and only the 65 cm^{-1} band is small and as the annealing temperature increases it becomes dominant displacing to higher frequencies. This fact corroborates that is not change of crystalline phase. The Raman spectroscopy can give a clearer evidence of the crystalline evolution in function of the annealed temperature and allows following the different steps if there is transformation by analysing the evolution of lowest frequency peaks (up to 100 cm^{-1}) of the Raman spectra. These peaks correspond to lattice modes of vibrational nature and are noticeably affected by the transition between the low symmetry phases of WO_3. Most vibrational peaks below of 200 cm^{-1} in the WO_3 Raman spectrum are attributed to lattice modes. As is observed in Fig. 4, only the peaks are enhanced with the annealing.

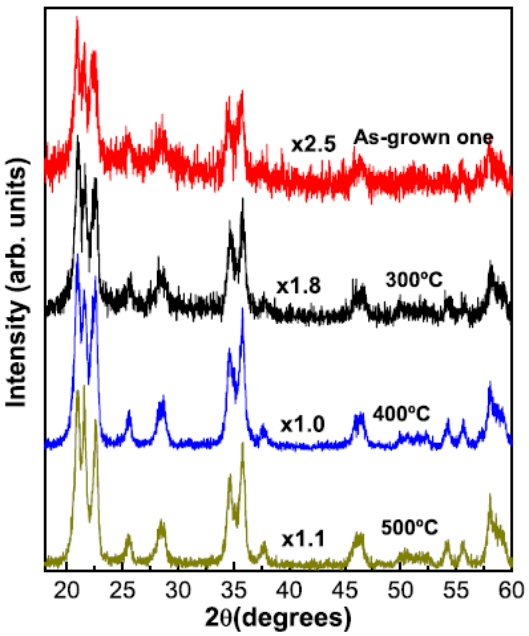

Fig.2. Fig. 2. XRD difractograms of WO_3 films deposited by heating resistive annealed at different temperatures.

Figure 3 shows the variations of the main Raman peaks as function of the annealed temperature, the behaviour of all ones is similar in the investigated temperature range, whose tendency is to increase. All the vibrational modes are slightly displaced toward higher frequencies with the annealed. D. Gazzoli [23] indicated that the vibrational bands positions in Raman spectrum depend on the tungsten content: at higher the W content, higher the frequency at which the band appears and the removal of water molecules causes a shift of the Raman bands at higher

frequency, as it was seen by XPS. There is a difference in our ex-situ Raman spectra before and after heat treatment. The peak at 801 cm^{-1} shifts slightly to higher frequency (811 cm^{-1}) after annealing. Due to above statements, the 811 cm^{-1} peak indicates that the WO_3 film contains more oxygen deficiency and the 801 cm^{-1} indicates more moisture on the film before annealing, which had been found by XPS measurements. Since it is an ex-situ measurement, even if we remove the surface water molecules of the film they can be partly absorbed on surface again during the experiment after annealing. Hence we deduced that the shift comes from the internal structure or phase of the film, not from the surface of the film.

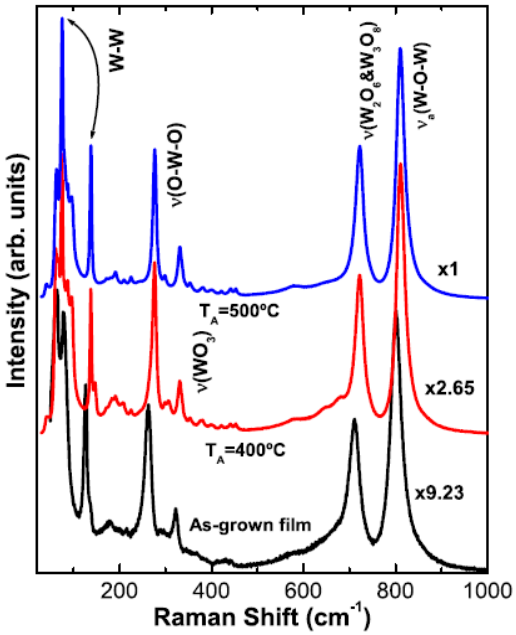

Fig. 3. Raman spectra of WO_3 thin films annealed at different temperatures.

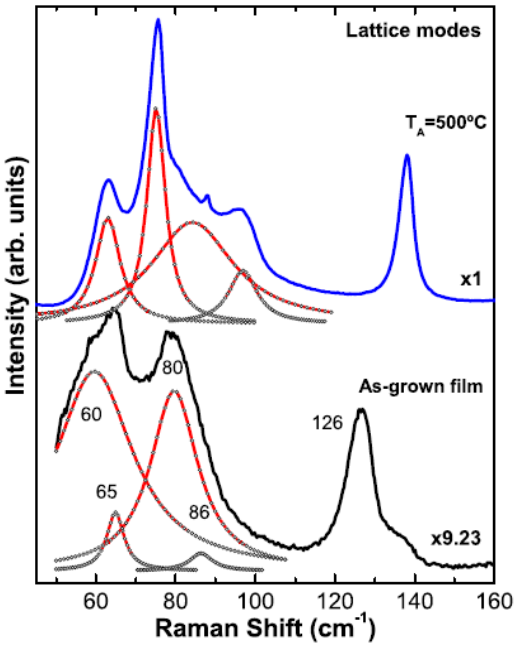

Fig. 4. Raman spectra of two WO_3 thin films at low frequencies: as-deposited and annealed at 500ºC.

All the above facts support the hypothesis of an open (or porous) structure of the films with many inner empty spaces and inter-grain boundaries. This means that comparably small amounts of water were absorbed in the films. The results suggest that the formation of porous films is due to gas-phase reactions in the plasma, leading to a homogeneous nucleation of oxide particles on the substrate. Clearly the prepared films were not a typical crystalline WO_3 (monoclinic phase or m-phase) structure. In addition probably an increase of compressive residual stress of the film due to annealing causes Raman shift to higher wavenumbers. This phenomenon has also been observed in IrO_2 films [24], ZrO2 films [25] and on the GaAs-SiO_2 interface [26]. Considering the residual stress and the Raman peak position before and after annealing, it can be concluded that the Raman peak position shifts to higher wavenumbers with the increase of compressive stress and it shifts to lower wavenumbers with the increase of tensile stress. To obtain a quantitative measurement of the residual stress of the WO_3 films, more detailed work is needed.

Figure 5 illustrates the 300 K photoluminescence of the as-deposited sample; it presents two radiative transitions sited at 2.35 and 2.65 eV that might be associated to oxygen vacancies, although the band A is more intense for the investigated annealing temperature range. As can see in Fig. 6, the band labelled by A does not change its radiative energy, however, the band B displaces towards high energies as the annealing temperatures is increased, as occurs with band gap. By transmittance measurements in the

visible and infrared range recorded for the WO_3 thin films before and after annealing allowed to obtain the optical band gap. The optical gap (E_g) was evaluated from the absorption coefficient (α) using the standard relation: $(\alpha h\nu)^{1/\eta} = A(h\nu - E_g)$, in which η depends on the kind of optical transition in semiconductors, and α was determined near the absorption edge using the simple relation: $\alpha = \ln[(1-R)^2/T]/d$, where d is the thickness of the film. The relationship between the optical band gap energy and the annealing temperature for WO_3 is shown in part upper of Fig. 6. As can be seen, the optical band gap for the as-deposited WO_3 is evaluated as 2.92 eV. The amorphous structure of the as-deposited WO_3 causes E_G to be bigger than 2.7 eV. After annealing the samples at 100°C, the optical band gap decreased slightly, by about 0.02 eV, which can be related to condensation of the films. However, the optical band gap of the WO_3 annealed at range from 200 to 500 C increased to 3.13 eV due to crystallization of the film. The reason E_G becomes bigger than 2.7 eV is the WO_3 crystallization and the oxygen vacancies at this temperature, as seen in Fig. 6. It is worth noting that for evaporated WO_3 films, one has found $2.7 < E_G < 3.5$ eV [1]. In the inset of Fig. 6 is shown the dependence of the radiative band intensity versus annealing temperature, as is observed they follow a dependence $I(T)\ \alpha\ T^a$, with $a_A=1.9x10^{-3}$ and $a_B=2.4x10^{-3}$.

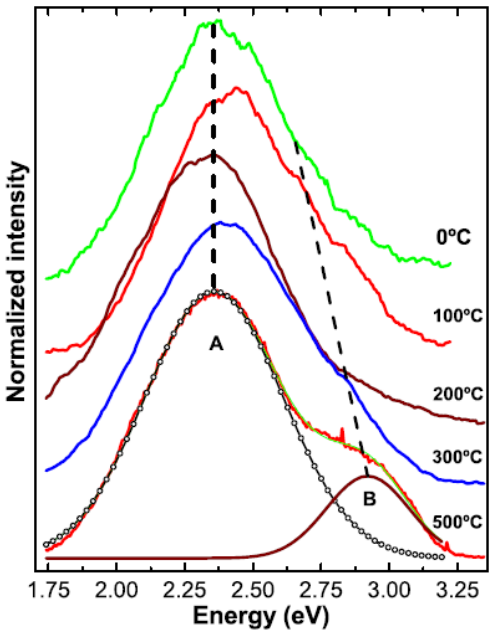

Fig. 5. Room-temperature photoluminescence of the WO_3 thin films as-deposited and annealed at different temperatures.

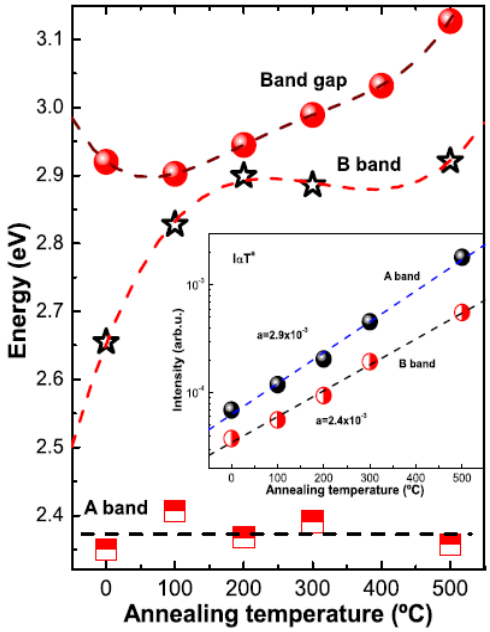

Fig. 6. Optical band gap energy of the WO_3 thin films as-deposited and annealed at different temperatures.

4 Conclusion

In this work has investigated the role of annealing temperature, as an external parameter, to control the optical and structural properties of WO_3 deposited by resistive heating. Using X-ray diffraction is obtained that WO_3 thin films only present as dominant phase the monoclinic and improved their structural quality with the annealing temperature up 400ºC and higher temperatures occurs the opposite by the lost of oxygen. By XPS measurements found that the WO_3 deposited is stoichiometric and with the annealing causes oxygen vacancies. The Raman spectroscopy indicates similar results, since the peak sited at 801 cm^{-1} shift to 811 cm^{-1} when it is annealed at 500ºC, this small change indicates a higher tungsten concentration that oxygen. Finally, by transmittance measurements is found that is possible vary the band gap energy between 2.92 to 3.12 annealed the samples.

References:

[1] C G Granqvist, *Handbook of Electrochromic Materials* (Amsterdam: Elsevier) **1995**.

[2] C. O. Avellaneda and L. O. S. Bulhões, *Solid State Ionics,* 165, **2003**, pp. 117.

[3] S. H. Lee, H. M. Cheong, P. Liu, D. Smith, C. Edwin Tracy, A. Mascanrenhas, J. R. Pitts and S. K. Deb, *Journal of Applied Physics,* 88, **2000**, pp. 3076.

[4] E. György, G. Socol, I. N. Mihailescu, C. Ducu and S. Ciuca, *Journal of Applied Physics,* 97, **2005**, pp. 093527.
[5] M. A. Gondal, A. Hameed, Z. H. Yamani and A. Suwaiyan, *Chemical Physics Letters,* 385, **2004**, pp. 111.
[6] M. Feng, A. L. Pan, H. R. Zhang, Z. A. Li, F. Liu, H. W. Liu, D. X. Shi, B. S. Zou and H. J. Gao, *Applied Physics Letters,* 86, **2005**, pp. 141901.
[7] R. Azimirad, O. Akhavan and A. Z. Moshfegh, *Journal of Electrochemical Society,* 153, **2006**, pp. E11.
[8] J. Hao, S. A. Studenikin and M. Cocivera, *Journal of Applied Physics,* 90, **2001**, pp. 5064.
[9] Y. Takeda, N. Kato, T. Fukano, A. Takeichi and T. Motohiro, *Journal of Applied Physics,* 96 (**2004**) 2417.
[10] G. Garcia-Belmonte, P. R. Bueno, F. Fabregat-Santiago and J. Bisquert, *Journal of Applied Physics,* 96, **2004**, pp. 853.
[11] M. Seman and C. A. Wolden, *Journal of Vacuum Science and Technology* A, 21, **2003**, pp. 1927.
[12] J. Díaz-Reyes, V. Dorantes-García, A. Pérez-Benítez and J. A. Balderas-López, *Superficies y Vacío,* 21, **2008**, pp. 12.
[13] C. G. Granqvist, *In The CRC Handbook of Solid State Electrochemistry*, Gellings, P. J.; Bouwmesster, H. J. M. eds.; CRC Press, Inc.: Cleveland Ohio, **1997**, ch. 16.
[14] P. R. Bueno, F. M. Pontes, E. R. Leite, L. O. S. Bulhões, P. S. Pizani, P. N. Lisboa-Filho, W. H. Schreiner, *Journal of Applied Phy*sics, 96**, 2004**, pp. 2102.
[15] M. F. Daniel, B. Desbat, J. C. Lassegues, R. Garie, *Journal of Solid State Chemical*, 73, **1988**, pp. 127.
[16] P. Tägtström, U. Jansson, *Thin Solid Films,* 352, **1999**, pp. 107.
[17] G. A. de Wijs, R. A. de Groot, *Electrochimica Acta*, 46, **2001**, pp. 1989.
[18] F. Daniel, B. Desbat, J. C. Lassegues, B. Gerand, M. Figlarz, *Journal of Solid State Chemical,* 67, **1987**, pp. 235.
[19] E. Salje, *Acta Crystallographic* A, 31, **1975**, pp. 360.
[20] A. Rougier, F. Portemer, A. Quédé, M. El Marssi, *Applied Surface Science,* 153, **1999**, pp. 1.
[21] M. Regragui, M. Addou, A. Outzourhit, J.C. Bernéde, Elb. El Idrissi, E. Benseddik, A. Kachouane, *Thin Solid Films,* 358, **2000**, pp. 40.
[22] J. V. Gabrusenoks, P. D. Cikmach, A.R. Lusis, J. J. Kleperis and G. M. Ramans, *Solid State Ionics,* 14, **1984**, pp., 25.
[23] D. Gazzoli, M. Valigi, R. Dragone, A. Marucci and G. Mattei, *Journal of Physics Chemical B,* 101, **1997**, pp. 11129.
[24] P. C. Liao, C. S. Chen, W. S. Ho, Y. S. Huang, and K. K. Tiong, *Thin Solid Films,* 301, **1997**, pp. 7.
[25] A. Portinha, V.Teixeira, J. Carneiro, M.F. Costa, N. P. Barradas, A. D. Sequeira, *Surface and Coatings Technology,* 188-189, **2004**, pp. 107.
[26] A. B. M. H. Rashid, M. Kishi, T. Katoda, *Journal of Applied Physics,* 80, **1996**, pp. 3540.